Mechanism of the Formation of Contractile Ring in Dividing Cultured Animal Cells. I. Recruitment of Preexisting Actin Filaments into the Cleavage Furrow

Long-guang Cao and Yu-li Wang

Cell Biology Group, Worcester Foundation for Experimental Biology, Shrewsbury, Massachusetts 01545

Abstract. Cytokinesis of animal cells involves the formation of the circumferential actin filament bundle (contractile ring) along the equatorial plane. To analyze the assembly mechanism of the contractile ring, we microinjected a small amount of rhodamine-labeled phalloidin (rh-pha) or rhodamine-labeled actin (rh-actin) into dividing normal rat kidney cells. rh-pha was microinjected during prometaphase or metaphase to label actin filaments that were present at that stage. As mitosis proceeded into anaphase, the labeled filaments became associated with the cortex of the cell. During cytokinesis, rh-pha was depleted from polar regions and became highly concentrated into the equatorial region. The distribution of total actin filaments, as revealed by staining the whole cell with fluorescein phalloidin, showed a much less pronounced difference between the polar and the equatorial regions. The sites of de novo assembly of actin filaments during the formation of the contractile ring were determined by microinjecting rh-actin shortly before cytokinesis, and then extracting and fixing the cell during mid-cytokinesis. Injected rhodamine actin was only slightly concentrated in the contractile ring, as compared to the distribution of total actin filaments. Our results indicate that preexisting actin filaments, probably through movement and reorganization, are used preferentially for the formation of the contractile ring. De novo assembly of filaments, on the other hand, appears to take place preferentially outside the cleavage furrow.

CYTOKINESIS of animal cells has attracted the attention of cell biologists for more than a century (for recent reviews see Rappaport, 1986; Mabuchi, 1986). However, its mechanism still remains unclear. Studies over the past twenty years have indicated that actin and myosin II are likely to be involved in this process. For example, actin filaments show a parallel, bundle-like arrangement in the cleavage furrow, forming a "contractile ring" (Perry et al., 1971; Forer and Behnke, 1972; Schroeder, 1973). Myosin II molecules exist as minifilaments in this region, and appear more concentrated than in other regions of the cell (Fujiwara and Pollard, 1976; Yumura and Fukui, 1985; Maupin and Pollard, 1986). Various observations indicate that the integrity of actin and myosin structures is crucial for cytokinesis. Cytochalasin B, which binds to the ends of actin filaments and may also induce filament breakage, inhibits cytokinesis with a concomitant disappearance of the contractile ring (Schroeder, 1970, 1972). The involvement of myosin II has been convincingly demonstrated with the microinjection of antibodies against myosin II (Mabuchi and Okuno, 1977; Kiehart et al., 1982), and with the disruption of myosin II expression after genetic manipulations (De Lozanne and Spudich, 1987; Knecht and Loomis, 1987). These treatments effectively inhibited cytokinesis while allowing karyokinesis to proceed.

However, many critical questions concerning the roles of actin and myosin in cytokinesis need to be clarified. Because the contractile ring is a transient structure, it is important to determine how actin and myosin filaments become organized and subsequently dissociated. One possibility for the formation of the contractile ring involves the de novo assembly of unpolymerized subunits onto nucleation sites along the equatorial plane. Alternatively, existing filaments may congregate into the cleavage furrow during cytokinesis. Information on the formation of contractile ring may also shed light on the mechanism of cell division. For example, cortical flow of actin filaments has been proposed in a model where contraction occurs throughout most cortical regions while relaxation takes place at the two poles (White and Borisy, 1983; Bray and White, 1988).

The purpose of this study is to identify the source of actin that becomes incorporated into the contractile ring. Normal rat kidney (NRK)[1] cells were microinjected during prometaphase or metaphase with rhodamine-labeled phalloidin (rh-pha), which became tightly associated with actin filaments present at that time. The distribution of rh-pha–labeled actin

1. *Abbreviations used in this paper*: fl-pha and rh-pha, fluorescein- and tetramethylrhodamine-labeled phalloidin, respectively; NRK, normal rat kidney; rh-actin, tetramethylrhodamine-labeled actin.

filaments was then followed until cytokinesis and was compared to the distribution of the total actin filaments as revealed by staining with fluorescein-labeled phalloidin (fl-pha). In a complementary experiment, the sites of de novo assembly were determined by microinjecting fluorescently labeled actin into cells shortly before the formation of the contractile ring, and extracting cells during mid-cytokinesis. Our results indicate that preexisting actin filaments are used preferentially for the formation of the contractile ring.

Materials and Methods

Fluorescent Phalloidin and Actin

rh-pha and fl-pha were purchased from Molecular Probes Inc. (Eugene, OR) as a 3.3-μM stock solution in methanol. In a typical experiment, 400 μl of the stock solution was removed and dried under N_2 and redissolved in 40 μl of 5 mM Tris-acetate buffer, pH 6.95. Thus the final concentration is 33 μM. The solution is clarified at 25,000 rpm for 20 min in a rotor (type 42.2 Ti; Beckman Instruments, Inc., Palo Alto, CA) before microinjection.

G-actin was purified and fluorescently labeled with tetramethylrhodamine as described previously (Wang, 1984). Tetramethylrhodamine-labeled actin (rh-actin) was microinjected at a concentration of 4–5 mg/ml.

Cells Culture and Microinjection

NRK epithelial cells (NRK-52E; American Type Culture Collection, Rockville, MD) were maintained in the F12K medium (Hazleton Systems, Inc., Lenexa, KS) containing 10% Nu-serum (Collaborative Research, Bedford, MA), 50 μg/ml streptomycin, and 50 μg/ml penicillin. Cells were plated onto special coverslip dishes for 36–48 h before microinjection (McKenna et al., 1989). Culturing of cells on the microscope stage during microinjection and observation was performed as described previously (McKenna et al., 1989).

Cells at various stages of mitosis were identified and microinjected. A tank of compressed air was used as the source of pressure for microinjection. The pressure was regulated with a custom-designed electronic control system. The solutions were microinjected conservatively, and the volume delivered was estimated to be <5% of the cell volume. No cell damage was visible under the phase optics, and microinjected cells divided normally, following a similar time course as did neighboring uninjected cells.

Staining of Cells with Fluorescent Phalloidin

Cells were rinsed twice with warm PHEM buffer (60 mM Pipes, 25 mM Hepes, pH 6.9, 10 mM EGTA, 2 mM $MgCl_2$; Schliwa and van Blerkom, 1981), and then extracted and fixed in two steps. The first step involved treatment with 1% formaldehyde (16% stock, EM grade; Electron Microscopy Sciences, Fort Washington, PA), 0.36% Triton X-100 in PHEM buffer, pH 6.1, for 2 min. This was followed by a 10-min treatment with 3.2% formaldehyde, 0.5% Triton X-100 in the same buffer. The dishes were then rinsed twice with the PHEM buffer, pH 6.9, and stained for 10 min with fluorescent phalloidin in the PHEM buffer at a concentration of 220 nM.

Fluorescence Microscopy and Image Processing

All observations were made with an inverted microscope (IM35; Carl Zeiss, Inc., Thornwood, NY) equipped with a 100×/NA 1.30 Neofluar objective and a 63×/NA 1.25 Neofluar objective. A 100-W quartz-halogen lamp, operated at 7 V or less, was used as the light source for epiillumination. This level of light, when applied intermittently, had no detectable effect on cell division.

Fluorescent images were detected with an ISIT low-light-level video camera (Dage-MTI Inc., Michigan City, IN), which was operated at a level far below saturation. Time-lapse sequences were recorded every 2–3 min. Images were processed by frame averaging and background subtraction. Bandpass filters were used for fluorescence observations, and no crossover between fluorescein and rhodamine was detectable. Paired video images were adjusted for registration by rapidly alternating the display between the two images. Misregistration appears as flickering. The position of one of the images was changed until no flickering was visible. For pseudocolor display, images were scaled to obtain a similar gray value at either the equatorial cortex (see Figs. 3–7) or the polar cortex (see Fig. 2). This facilitates the comparison of different images. Black-and-white images were photographed off a video monitor as described previously (McKenna et al., 1989). Color images were photographed off a monitor (model PVM-1271Q; Sony Corp. of America, New York) with film (Gold 400; Eastman Kodak Co., Rochester, NY) and processed in a commercial studio.

Results

Changes in the Distribution of Rh-pha–labeled Actin Filaments during Cell Division

To observe the distribution of actin filaments during cell division, we microinjected a trace amount of rh-pha into prometaphase or metaphase NRK cells, an epithelial cell line that remains well spread during mitosis. The microinjection induced no detectable changes in cellular morphology or in the time course of mitosis.

A series of rh-pha images from a cell typical of over 30 cells observed was shown in Fig. 1. Rh-pha was initially concentrated as a spot near the site of microinjection, but gradually spread throughout the cell over 10–20 min, suggesting that it associated rapidly with actin filaments and was not freely diffusible in the cytoplasm. Moreover, the intensity and distribution of rh-pha showed no detectable change after extraction and fixation. During metaphase, rh-pha assumed a relatively uniform distribution except for the site of injection and the regions of chromosomes (Fig. 1 *a*). During anaphase, when sister chromosomes were moving toward opposite poles, rh-pha became concentrated onto the cell cortex (Fig. 1 *b*). However, no consistent difference between the polar and equatorial cortices was observed at this point.

A gradual concentration of rh-pha along the equatorial plane was observed 2–5 min before the onset of cytokinesis. The equatorial fluorescence intensity reached a peak during mid-cytokinesis (Fig. 1 *c*), such that all microinjected cells showed a dramatic concentration of fluorescence. Intensity near the poles underwent a concomitant decrease during cytokinesis, and the polar edge of the cell often became undetectable in the fluorescence images. Upon the completion of cytokinesis, rh-pha became gradually relocated to nascent stress fibers and the polar cortex (not shown).

Comparison of the Distribution of Preexisting Actin Filaments and Total Actin Filaments during Cytokinesis

To compare the distribution of rh-pha–labeled filaments with that of total actin filaments, uninjected cells undergoing cytokinesis were fixed and stained with rh-pha to reveal the distribution of total actin filaments. Fluorescence at the polar and the equatorial cortices was compared after normalizing the average intensity at the polar regions of different cells. Pseudocolor display was used to facilitate the visualization of differences. The cells were categorized according to the color in the cleavage furrow. 34% of the cells showed undetectable or only a slight increase in fluorescence on the equatorial plane relative to the poles (no difference in color, Fig. 2 *a*; Fig. 7 *b* also belongs to this category). More than half of the cells (52%) showed a moderate increase in equatorial fluorescence relative to the polar fluorescence (slight difference in color display, Fig. 2 *b*; Figs. 3 *b*, 5 *b*, and 6 *b* also belong to this category), and only about 14%

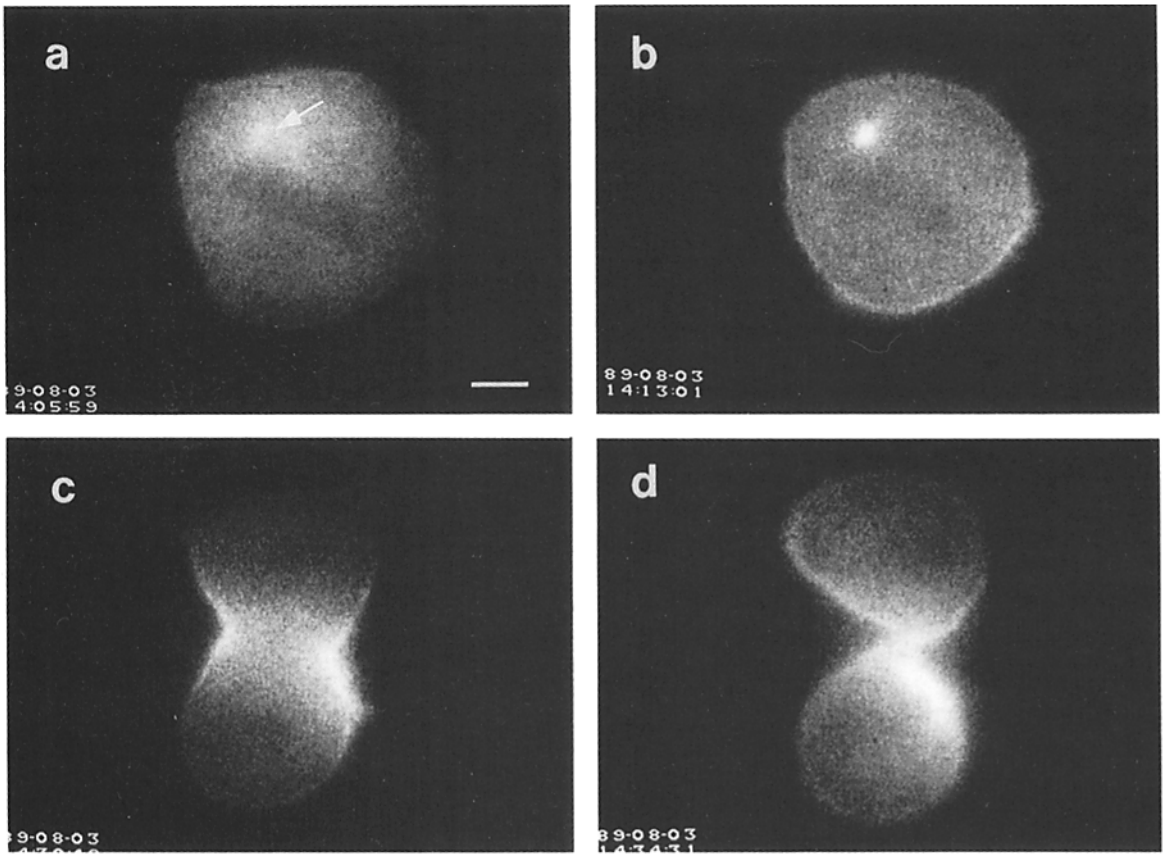

Figure 1. Changes in the distribution of microinjected rh-pha in a living NRK cell during cell division. 2 min after microinjection into a metaphase cell (*a*), rh-pha is concentrated at the site of microinjection (*arrow*) and depleted from the region where chromosomes are located. Otherwise, the distribution of fluorescence appears uniform in the cell. 7 min later, at early anaphase (*b*), the membrane cortex starts to show an increase in fluorescence intensity. During mid-cytokinesis (*c*), rh-pha becomes highly concentrated along the equatorial plane. Cytokinesis is essentially completed 3 min later (*d*), and rh-pha slowly spreads out from the equatorial plane. Bar, 5 μm.

showed a dramatic concentration of fluorescence (Fig. 2 *c*; Fig. 4 *b* also belongs to this category). However, when microinjected rh-pha was viewed in this fashion, all cells showed a dramatic concentration at the cleavage furrow relative to the poles (Fig. 2 *d*). The polar cortex was clearly visible in all stained cells (Fig. 2, *a–c*) but not in microinjected cells (Figs. 1 *c* and 2 *d*).

Direct comparison between the distribution of rh-pha–labeled filaments and that of total actin filaments was achieved by microinjecting cells with rh-pha at prometaphase, and then fixing, extracting, and staining the microinjected cells with fl-pha during cytokinesis (after >1 h incubation). The ratio image between the rhodamine and fluorescein images revealed, to a first approximation, the percentage of actin filaments that were labeled with injected rh-pha in different regions of the cell.

As shown in Fig. 3, injected rh-pha showed a striking difference between the polar and equatorial regions (Fig. 3 *a*). A more uniform distribution along the cortex was observed in the image of fl-pha staining (Fig. 3 *b*). The ratio image (Fig. 3 *c*) showed a higher value in the cleavage furrow, suggesting that the cleavage furrow contained a higher percentage of preexisting filaments that were labeled immediately after microinjection at prometaphase. The pattern and level of fl-pha staining of injected cells were similar to those of uninjected cells as shown in Fig. 2, *a–c*, indicating that the injection of rh-pha did not induce a change in the overall distribution of actin filaments.

To ensure that the results were not caused by instrumental artifacts, such as the limited linearity of the ISIT camera, cells were stained with a mixture of fl-pha and rh-pha. The images of the two fluorophores were indistinguishable (Fig. 4), and the ratio images showed a uniform distribution over the entire cell.

As a second control, cells were microinjected with rh-pha during cytokinesis, and then fixed and stained within 2–3 min of microinjection. In this case rh-pha should label actin filaments that were already organized for cytokinesis and should show a similar distribution to that of fl-pha staining. As shown in Fig. 5, there is little difference between the equatorial region and polar region in the lower half of the cell where rh-pha was microinjected. The upper half showed little fluorescence of rh-pha because of the limited diffusion within the short period of incubation.

Localization of the Site of Incorporation of Actin Subunits during Cytokinesis

We microinjected NRK cells with rhodamine-labeled actin subunits at anaphase, shortly before the onset of cytokinesis.

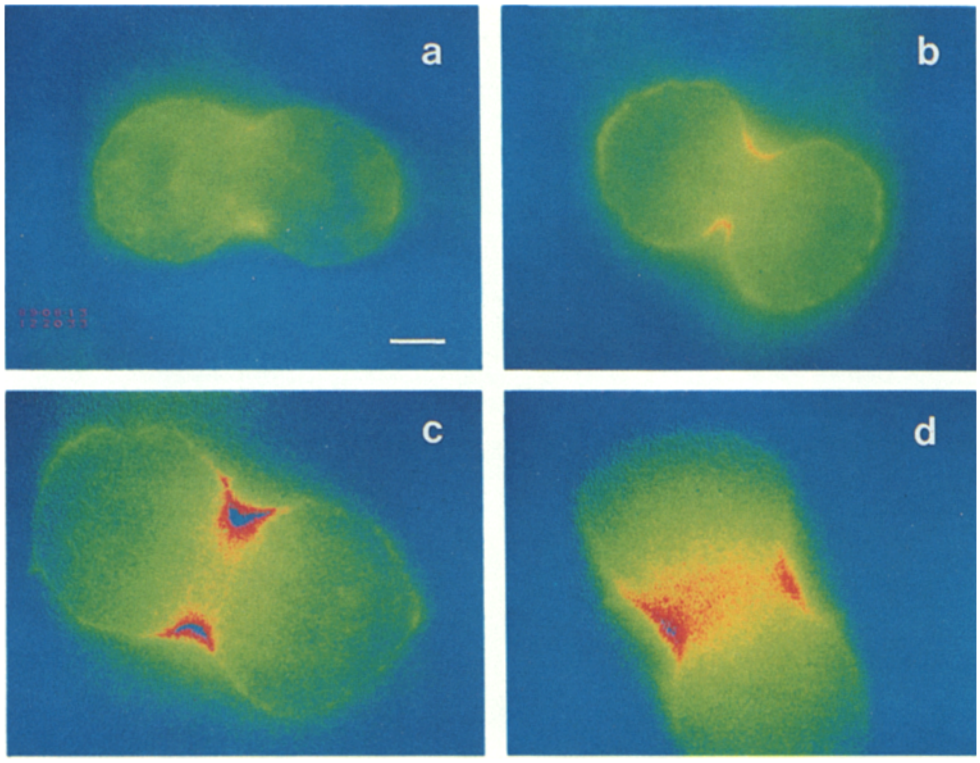

Figure 2. Difference between the distribution of microinjected rh-pha and rh-pha applied to fixed and extracted cells. Uninjected NRK cells during mid-cytokinesis were fixed, extracted, and stained with rh-pha (*a–c*). The extent of concentration of rh-pha on the equatorial plane relative to the poles varies from cell to cell. Many cells (~34%) show either no detectable or a very slight concentration of rh-pha in the cleavage furrow (*a*). About 52% show a clear, but limited concentration of rh-pha (*b*). Only ~14% of the cells show a dramatic concentration of rh-pha (*c*). Rh-pha microinjected during prometaphase or metaphase, on the other hand, shows a dramatic concentration in the cleavage furrow in 100% of the cells (*d*). The cortex in the polar region is clearly detectable in all fixed cells stained with rh-pha, but not in living cells microinjected with rh-pha. The range of gray scale is adjusted proportionally to obtain a similar level at the pole. The categorization of cells is based on pseudocolor display. The color changes in the order of blue-green-yellow-orange-red-blue with increasing intensities. Bar, 5 μm.

Injected cells were incubated (for 10–15 min) until mid-cytokinesis and were extracted, fixed, and stained with fl-pha to reveal the distribution of total actin filaments. The rhodamine fluorescence revealed the distribution of injected actin subunits that became incorporated into Triton-resistant structures during the formation of the contractile ring.

Before extraction and fixation, the distribution of rh-actin was relatively uniform, with no discernible concentration along the cortex (not shown). This is most likely due to the presence of a high concentration of unpolymerized actin in the cytoplasm. After extraction, a concentration of injected actin along the cortex became discernible (Fig. 6 *a*). The equatorial region showed a slightly higher level of fluorescence. However, after normalizing against total actin filaments, the equatorial region had a lower ratio than other regions of the cell (Fig. 6 *c*), indicating that the cleavage furrow contained a lower percentage of newly assembled actin filaments. When rhodamine actin was microinjected at

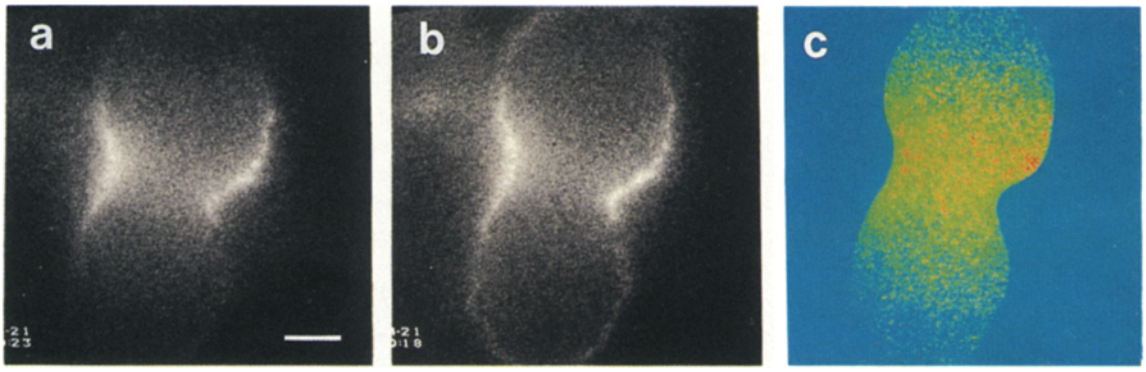

Figure 3. Concentration of rh-pha into the cleavage furrow after microinjection into prometaphase cells. An NRK cell was microinjected with rh-pha away from the equatorial plane during prometaphase and then incubated until mid-cytokinesis. The cell was extracted, fixed, and stained with fl-pha (*b*). In the image of rh-pha (*a*), the extent of concentration on the equatorial plane is much more pronounced whereas the polar regions are almost undetectable. The ratio image between rh-pha and fl-pha shows a higher value in the cleavage furrow (*c*). Pseudocolor display is performed as in Fig. 2. The ratio is scaled to obtain green color in the cortex of cleavage furrow. A similar procedure is used for the pseudocolor display in Figs. 4–7. Bar, 5 μm.

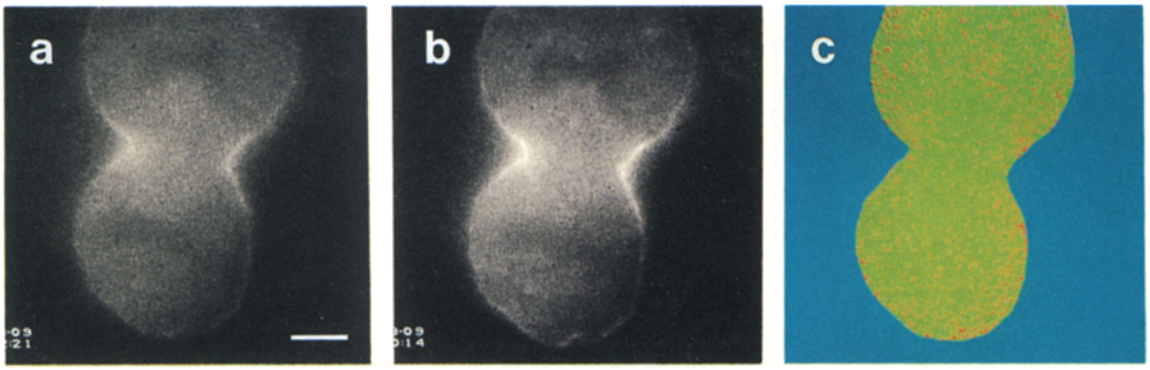

Figure 4. Identical distribution of rh-pha (*a*) and fl-pha (*b*) when the two were applied simultaneously to extracted, fixed NRK cells. The ratio image (*c*) shows no difference between the polar and equatorial regions. Bar, 5 μm.

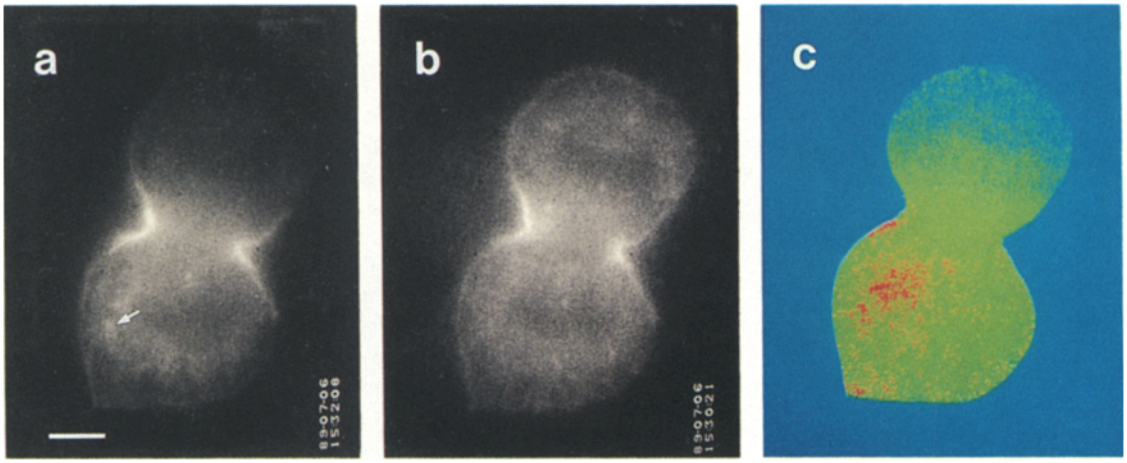

Figure 5. Distribution of rh-pha microinjected during cytokinesis. A telophase NRK cell was microinjected with rh-pha and, after 3 min, was extracted, fixed, and stained with fl-pha (*b*). Image of rh-pha (*a*) shows labeling of the cortex and concentration in the cleavage furrow. The upper polar region, which is far away from the site of microinjection, shows little fluorescence because of the slow spreading of rh-pha. The ratio image between *a* and *b* indicates similar values in the cleavage furrow and near the lower pole *c*. A higher ratio is seen at the site of microinjection (*arrow*). Bar, 5 μm.

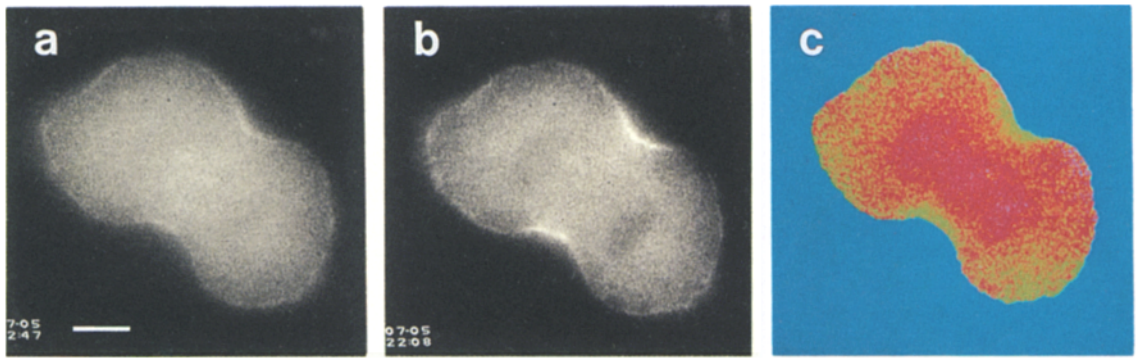

Figure 6. Sites of incorporation of rh-actin microinjected shortly before cytokinesis. Mid-cytokinesis was reached 15 min after microinjection. The cell was extracted, fixed, and stained with fl-pha (*b*). Rh-actin shows a slight concentration in the cleavage furrow (*a*). However, after normalizing against the image of fl-pha by taking the ratio, the extent of incorporation in the equatorial region appears lower than that in polar regions (*c*). Bar, 5 μm.

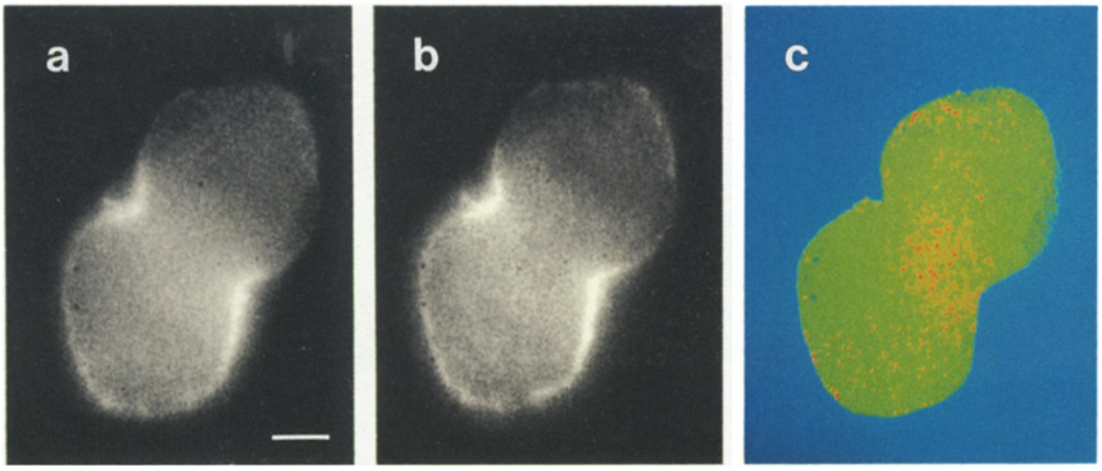

Figure 7. Distribution of microinjected rh-actin during cytokinesis after an extended period of incubation. An NRK cell was microinjected with rh-actin during metaphase and was incubated until mid-cytokinesis (>1 h). The cell was extracted, fixed, and stained with fl-pha (*b*). The distribution of rh-actin and fl-pha is very similar, and the ratio image (*c*) shows no difference between the poles and the cleavage furrow. Bar, 5 μm.

prometaphase and cells incubated until cytokinesis (>1 h), the distribution of rhodamine became very similar to that of fl-pha staining (Fig. 7).

Discussion

One of the central questions about cytokinesis is the mechanism of the formation of the contractile ring. So far little information is available to allow the distinction between two possible models: de novo polymerization of actin filaments, and reorganization of existing actin filaments.

We have microinjected rh-pha and rh-actin into mitotic cells to label actin filaments. rh-pha should bind to actin filaments that are present at the time of microinjection, allowing us to follow the fate of these preexisting actin filaments through cytokinesis. On the other hand, rh-actin should become associated with actin filaments that are assembled after microinjection or with filaments that undergo active subunit exchange. Thus, if de novo assembly is the primary mechanism for the formation of the contractile ring, rh-actin microinjected shortly before cytokinesis should become concentrated into the contractile ring (relative to the distribution of total actin filaments), but rh-pha microinjected during metaphase should not be concentrated. On the other hand, if the contractile ring is formed by the reorganization of existing filaments, then opposite results should be obtained.

One important assumption in our experiment is that the injection of rh-pha does not affect the mechanism of cytokinesis. This is supported by the normal morphology of injected cells and their normal progression through mitosis. In addition, previous studies indicated no detectable perturbation when a tracer amount of phalloidin was microinjected into interphase cultured cells (Wehland and Weber, 1981; Wang, 1987). In the present study, the final concentration of the injected rh-pha is estimated to be 1–2 μM. Thus, only a small percentage of actin subunits in the filaments could be labeled, assuming that a cell contains ~100 μM actin in the filamentous form. This level of labeling should also have little effect on the subsequent staining of the cells with fl-pha. It is possible that some filaments or segments of filaments could be stabilized by the injected rh-pha (Wieland, 1977), and undergo reduced subunit on–off reactions. However, whether this is the case or not, both the time course of cytokinesis and the distribution of total actin filaments appear unaffected by the microinjection. Thus, it is unlikely that the observed concentration of rh-pha–labeled filaments into the cleavage furrow represents a phalloidin-induced event.

The simplest explanation of our results is that the contractile ring is formed primarily by the reorganization of existing actin filaments, although it is difficult to rule out entirely the involvement of de novo assembly. According to the time course shown in Fig. 1, it is likely that actin filaments are uniformly distributed in the cytoplasm during metaphase. At anaphase, some filaments become associated with the cell cortex, as has been observed for both actin and myosin II in fixed and stained *Dictyostelium* cells (Kitanishi-Yumura and Fukui, 1989). During cytokinesis, existing actin filaments are concentrated into the equatorial plane (Fig. 1), while new actin filaments may be assembled in other areas such as polar regions.

The behavior of actin during cytokinesis described here is in sharp contrast to that observed at the leading lamellipodia. Labeled G-actin becomes rapidly concentrated into the lamellipodia after microinjection (Glacy, 1983), whereas microinjected rh-pha fails to label this region (Wehland and Weber, 1981; Wang, 1987). These observations are consistent with the constant formation of new actin filaments in the lamellipodia (Wang, 1985). Thus, it is likely that there are two different pathways for the formation of actin-rich structures: one involving de novo assembly and the other involving reorganization of existing filaments.

While preexisting filaments are consistently depleted from the polar regions and highly concentrated in the cleavage furrow, the distribution of total filamentous actin appears much more uniform along the cortex (Fig. 2). In cells microinjected with fluorescent actin, the concentration of actin filaments within the cleavage furrow cannot be discerned until cells are extracted (Wang and Taylor, 1979; Fig. 7), most likely because of the presence of a high concentration of soluble subunits in the cytoplasm. The extent of actin con-

centration in the cleavage furrow has been a matter of controversy. Although some studies indicated a high degree of concentration (e.g., Sanger, 1975; Aubin et al., 1979), others reported no consistent concentration (Herman and Pollard, 1979; Hamaguchi and Mabuchi, 1982). The results were no doubt affected by the methods of sample preparation and the specificity of the staining agents (recognizing F-actin only or both G- and F-actin). Our results indicate that the distribution of total actin filaments, as indicated by staining fixed cells with fluorescent phalloidin, varies considerably among dividing cells. While some cells (~14%) show a dramatic concentration of actin filaments in the cleavage furrow relative to the poles (Fig. 2 *c*), others (~34%) exhibit either undetectable or only a slight difference between the equatorial and polar cortices (Fig. 2 *a*). However, most cells show a moderate extent of concentration of rh-pha in the cleavage furrow, while the polar cortex remains detectable throughout cytokinesis (Fig. 2 *b*). Because similar distributions are observed with live cells microinjected with rh-pha during cytokinesis, the results are unlikely to represent artifacts of extraction and fixation. In addition, the pattern of phalloidin staining in most cells is similar to that observed in dividing *Dictyostelium* cells (Kitanishi-Yumura and Fukui, 1989). Several other proteins, including filamin and alpha-actinin, also show a variable degree of concentration in the cleavage furrow (Nunnally et al., 1980), indicating that a high degree of concentration of these contractile proteins is not required for cytokinesis.

At least two mechanisms should be considered for the concentration of existing actin filaments into the cleavage furrow. First, actin filaments in the contractile ring may be recruited from the cytoplasm. During cytokinesis, the affinity or the number of binding sites for actin filaments may increase in the equatorial region. The depletion of rh-pha from polar areas may be explained if actin filaments undergo constant on–off reactions along the membrane, and are thus capable of rapid redistribution according to the distribution or affinity of binding sites. In the second mechanism, membrane-associated filaments may move toward the cleavage furrow as part of the "cortical flow" as suggested previously (White and Borisy, 1983; Bray and White, 1988). Such a flow may originate at the polar region, resulting in a severe depletion of preexisting filaments from poles. One interesting question would then be the relative movement of actin and myosin II molecules, which have also been observed to concentrate in the cleavage furrow (Fujiwara and Pollard, 1976; Mittal et al., 1987; Sanger et al., 1989). If the mechanism of flow involves actin–myosin interactions, one might expect myosin and actin filaments to move relative to each other in opposite directions.

To distinguish between the two models, it would be important to observe directly the movement of actin filaments before and during cytokinesis. Because there are few discrete actin-containing structures in mitotic cells to allow direct tracking of filaments, approaches such as fluorescence photobleaching may be useful in marking specific spots whose translocation can then be studied.

We would like to thank M. C. Sanders and Dr. Richard Vallee for reading this manuscript.

The research is supported by National Institutes of Health grant GM-32476.

Received for publication 2 October 1989 and in revised form 1 December 1989.

References

Aubin, J. E., K. Weber, and M. Osborn. 1979. Analysis of actin and microfilament-associated proteins in the mitotic spindle and cleavage furrow of PtK2 cells by immunofluorescence microscopy. *Exp. Cell Res.* 124:93–109.

Bray, D., and J. G. White. 1988. Cortical flow in animal cells. *Science (Wash. DC).* 239:883–888.

De Lozanne, A., and J. A. Spudich. 1987. Disruption of *Dictyostelium* myosin heavy chain gene by homologous recombination. *Science (Wash. DC).* 236:1086–1091.

Forer, A., and O. Behnke. 1972. An actin-like component in spermatocytes of a crane fly *(Nephrotoma suturalis* Loew). II. The cell cortex. *Chromosoma (Berl.).* 39:175–190.

Fujiwara, K., and T. D. Pollard. 1976. Fluorescent antibody localization of myosin in the cytoplasm, cleavage furrow, and mitotic spindle of human cells. *J. Cell Biol.* 71:848–875.

Glacy, S. D. 1983. Subcellular distribution of rhodamine-actin microinjected into living fibroblastic cells. *J. Cell Biol.* 97:1207–1213.

Hamaguchi, Y., and I. Mabuchi. 1982. Effects of phalloidin microinjection and localization of fluorescein-labeled phalloidin in living sand dollar eggs. *Cell Motil.* 2:103–113.

Herman, I. M., and T. D. Pollard. 1979. Comparison of purified anti-actin and fluorescent-heavy meromyosin staining patterns in dividing cells. *J. Cell Biol.* 80:509–520.

Kiehart, D. P., I. Mabuchi, and S. Inoue. 1982. Evidence that myosin does not contribute to force production in chromosome movement. *J. Cell Biol.* 94:165–178.

Kitanishi-Yumura, T., and Y. Fukui. 1989. Actomyosin organization during cytokinesis: reversible translocation and differential redistribution in *Dictyostelium. Cell Motil. Cytoskeleton.* 12:78–89.

Knecht, D. A., and W. F. Loomis. 1987. Antisense RNA inactivation of myosin heavy chain gene expression in *Dictyostelium discoideum. Science (Wash. DC).* 236:1081–1086.

Mabuchi, I. 1986. Biochemical aspects of cytokinesis. *Int. Rev. Cytol.* 101:175–213.

Mabuchi, I., and M. Okuno. 1977. The effect of myosin antibody on the division of starfish blastomeres. *J. Cell Biol.* 74:251–263.

Maupin, P., and T. D. Pollard. 1986. Arrangement of actin filaments and myosin-like filaments in the contractile ring and of actin-like filaments in the mitotic spindle of dividing HeLa cells. *J. Ultrastruct. Mol. Struct. Res.* 94:92–103.

McKenna, N. M., Y.-L. Wang, and M. E. Konkel. 1989. Formation and movement of myosin-containing structures in living fibroblasts. *J. Cell Biol.* 109:1163–1172.

Mittal, B., J. M. Sanger, and J. W. Sanger. 1987. Visualization of myosin in living cells. *J. Cell Biol.* 105:1753–1760.

Nunnally, M. H., J. M. D'angelo, and S. W. Craig. 1980. Filamin concentration in cleavage furrow and midbody region: frequency of occurrence compared with that of alpha-actinin and myosin. *J. Cell Biol.* 87:219–226.

Perry, M. M., H. A. John, and N. S. T. Thomas. 1971. Actin-like filaments in the cleavage furrow of newt egg. *Exp. Cell Res.* 65:249–253.

Rappaport, R. 1986. Establishment of the mechanism of cytokinesis in animal cells. *Int. Rev. Cytol.* 105:245–281.

Sanger, J. W. 1975. Changing patterns of actin localization during cell division. *Proc. Natl. Acad. Sci. USA.* 72:1913–1916.

Sanger, J. M., B. Mittal, J. S. Dome, and J. W. Sanger. 1989. Analysis of cell division using fluorescently labeled actin and myosin in living PtK2 cells. *Cell Motil. Cytoskeleton.* 14:201–219.

Schliwa, M., and J. van Blerkom. 1981. Structural interaction of cytoskeletal components. *J. Cell Biol.* 90:222–235.

Schroeder, T. E. 1970. The contractile ring. I. Fine structure of dividing mammalian (HeLa) cells and the effects of cytochalasin B. *Z. Zellforsch. Mikrosk. Anat.* 109:431–449.

Schroeder, T. E. 1972. The contractile ring. II. Determining its brief existence, volumetric changes, and vital role in cleaving *Arbacia* eggs. *J. Cell Biol.* 53:419–434.

Schroeder, T. E. 1973. Actin in dividing cells: contractile ring filaments bind heavy meromyosin. *Proc. Natl. Acad. Sci. USA.* 70:1688–1692.

Wang, Y.-L. 1984. Reorganization of actin filament bundle in living fibroblasts. *J. Cell Biol.* 99:1478–1485.

Wang, Y.-L. 1985. Exchange of actin subunits at the leading edge of living fibroblasts: possible role of treadmilling. *J. Cell Biol.* 101:597–602.

Wang, Y.-L. 1987. Mobility of filamentous actin in living cytoplasm. *J. Cell Biol.* 105:2811–2816.

Wang, Y. L., and D. L. Taylor. 1979. Distribution of fluorescently labeled actin in living sea urchin eggs during early development. *J. Cell Biol.* 82:672–679.

Wehland, J., and K. Weber. 1981. Actin rearrangement in living cells revealed by microinjection of fluorescent phalloidin derivative. *Eur. J. Cell Biol.* 24:176–183.

White, J. G., and G. G. Borisy. 1983. On the mechanisms of cytokinesis in animal cells. *J. Theor. Biol.* 101:289–316.

Wieland, T. 1977. Modification of actins by phallotoxins. *Naturwissenschaften.* 64:303–309.

Yumura, S., and Y. Fukui. 1985. Reversible cyclic AMP-dependent change in distribution of myosin thick filaments in *Dictyostelium. Nature (Lond.).* 314:194–196.